Analytica Chimica Acta 707 (2011) 135–141

Contents lists available at SciVerse ScienceDirect

Analytica Chimica Acta

journal homepage: www.elsevier.com/locate/aca

A dual enzymatic-biosensor for simultaneous determination of glucose and cholesterol in serum and peritoneal macrophages of diabetic mice: Evaluation of the diabetes-accelerated atherosclerosis risk

Qilin Huang[a], Yarui An[a], Linlin Tang[a], Xiaoli Jiang[a], Hua Chen[a], Wenji Bi[a], Zhongchuan Wang[b], Wen Zhang[a,*]

[a] Department of Chemistry, East China Normal University, Shanghai 200062, PR China
[b] Department of Anorectal Surgery, Xinhua Hospital, Affiliated to School of Medicine of Shanghai Jiaotong University, Shanghai 200092, PR China

ARTICLE INFO

Article history:
Received 10 May 2011
Received in revised form 7 September 2011
Accepted 8 September 2011
Available online 16 September 2011

Keywords:
Glucose
Cholesterol
Simultaneous determination
Diabetes-accelerated atherosclerosis risk

ABSTRACT

In this paper, a novel dual enzymatic-biosensor is described for simultaneous determination of glucose and cholesterol in serum and peritoneal macrophages (PMs) of diabetic mice to evaluate the risk of diabetes-accelerated atherosclerosis. The biosensor was constructed by a three-step method. First, a poly-thionine (PTH) film was assembled on the surface of glassy carbon electrode by cyclic voltammetric electropolymerization of thionine, which serves as an electron transfer mediator (ETM). Second, gold nanoparticles (GNPs) were covered on the surface of PTH facilitating the electron transfer between glucose oxidase (GOx), cholesterol oxidase (ChOx) and electrode. Finally, the enzymes, GOx, cholesterol esterase (ChE), and ChOx, were covalently attached to the PTH layer through a chitosan (CH) linker. The PTH coupled with GNPs provides good selectivity, high sensitivity and little crosstalk for the dual enzymatic-biosensor. The developed biosensor had good electrocatalytic activity toward the oxidations of glucose and cholesterol, exhibiting a linear range from 0.008 mM to 6.0 mM for glucose with a detection limit of 2.0 μM, and a linear range from 0.002 mM to 1.0 mM for cholesterol with a detection limit of 0.6 μM. The results of the diabetic mice demonstrated that the cholesterol level did not change obviously with the increase of glucose level in serum, while the cholesterol level was induced with the increase of the glucose level in PMs. Previous studies have shown that the large accumulation of cholesterol in macrophage could lead to macrophage foam cell formation, which is the hallmark of early atherosclerosis. This study provides useful further evidences for the development of diabetes-accelerated atherosclerosis.
© 2011 Elsevier B.V. All rights reserved.

1. Introduction

Atherosclerosis is a chronic inflammatory disease characterized by narrowing of arteries caused by cholesterol-rich plaques of immune system cells [1,2]. It has been reported that atherosclerosis is the most common cause of morbidity and mortality in diabetic patients, and more precisely, more than 65% of death among diabetics results from atherosclerosis and its complications [3]. Previous studies have hypothesized that high blood glucose induced by diabetes can accelerate the risk of atherosclerosis, but the precise mechanisms underlying the acceleration of atherosclerosis in diabetes are poorly understood. Recently, some studies have shown that high glucose can lead to increased macrophage cholesterol accumulation in mice, and the large accumulation of cholesterol in macrophage is one of the main causes of atherosclerosis [4,5]. These results strongly suggest that high level of glucose in diabetes might accelerate the risk of atherosclerosis via induction of increased macrophage cholesterol accumulation. Therefore, the development of an effective method for simultaneous determination of glucose and cholesterol in serum and peritoneal macrophages (PMs) could clarify their relationship in the development of diabetes-accelerated atherosclerosis and has indispensable value in the study of atherosclerosis etiology.

Up to now, a variety of methods have been developed for blood glucose or cholesterol assays such as amperometry, spectrophotometry, electrochemical method, and high performance liquid chromatography (HPLC) [6,7]. Among these methods, enzyme-modified electrochemical biosensor is a promising tool since it can offer an improvement in terms of selectivity and sensitivity [8,9]. Glucose sensor is usually based on the selective enzymatic reaction of glucose oxidase (GOx), and cholesterol sensor involves cholesterol esterase (ChE) together with cholesterol oxidase (ChOx). Both biosensors can convert the corresponding substrates to hydrogen peroxide (H_2O_2), and the redox property of H_2O_2 can be used to

* Corresponding author. Fax: +86 21 6223 2627.
E-mail address: wzhang@chem.ecnu.edu.cn (W. Zhang).

0003-2670/$ – see front matter © 2011 Elsevier B.V. All rights reserved.
doi:10.1016/j.aca.2011.09.003

constitute a protocol for its electrochemical determination [10]. However, due to the slow kinetics, the redox process of H_2O_2 generally suffers from the interference from the oxidations of some compounds existing in blood and cells [11]. To accelerate the electron transfer rate, one of the most effective methods is to use an electron transfer mediator (ETM) taking place of O_2/H_2O_2 for the oxidase to realize the direct electron transfer between the enzyme redox center and the electrode. In various selective ETMs, some redox dyes of phenazine and phenothiazine derivatives exhibit fast reversible electrochemical response at negative potentials and can work as redox mediators for glucose and cholesterol sensors [12]. Normally, the second-generation biosensor using ETM suffer from two common drawbacks, insensitivity and low storage stability [13,14]. In recent years, with the remarkable development in biochemistry and nanotechnology, a great progress has been made in biosensors based on nanomaterials because of their unique signal amplifications and excellent electrocatalytic effects. The application of nanomaterials can enhance main performance parameters of biosensor, such as sensitivity and stability [15]. For example, platinum nanoparticles and SiO_2 nanoparticles have been used in glucose sensor for the immobilization of GOx to retain the protein bioactivity and enhance the sensitivity [16]. Laponite clay nanoparticles have been used in cholesterol sensor to improve the analytical performance of the biosensor in stability and storage stability [17,18].

In this paper, a novel dual enzymatic-biosensor was fabricated for simultaneous determination of glucose and cholesterol in serum and PMs of diabetic mice. For glucose sensor, the linear relationship was obtained in the range of 0.008–6.0 mM and the detection limit was calculated to be 2.0 μM, and for cholesterol sensor, the linear relationship was from 0.002 mM to 1.0 mM and the detection limit was 0.6 μM. The established method was successfully employed to determine the glucose and cholesterol of serum and PMs in diabetic mice and non-diabetic mice (control groups). The data obtained from diabetic mice indicated that the cholesterol level had no significant change when the glucose level was increased in serum. In contrast, the cholesterol level was induced with the increase of the glucose level in PMs. This effect can induce the formation of macrophage foam cell, which further accelerates atherosclerosis development [19–21]. These different changes suggest that outwardly unrelated status between glucose and cholesterol levels in diabetic serum perhaps hide the risk of early atherosclerotic, and the cooperative change of glucose and cholesterol levels in diabetic PMs is associated with the diabetes-accelerated atherosclerosis process.

2. Experimental

2.1. Chemicals

Glucose oxidase (GOx, EC 1.1.3.4, type II from *Aspergillus niger*), cholesterol oxidase (ChOx, EC 1.1.3.6, from *Streptomyces* sp.), cholesterol esterase (ChE, EC 3.1.1.13, from *Pseudomonas* sp.), glucose, cholesterol, cholesteryl oleate (97%), thionine, chitosan (CH), uric acid (UA), ascorbic acid (AA), streptozocin (STZ) were purchased from Sigma Chemical (St. Louis, MO, USA). Chloroauric acid ($HAuCl_4$), trisodium citrate, Triton X-100, isopropanol, trichloroacetic acid (TCA) were obtained from Sinopharm Chemical Reagent Co. Ltd. (Shanghai, China). GNPs were prepared according to the previous protocol by adding a trisodium citrate solution to a boiling $HAuCl_4$ solution [22]. 0.1 M phosphate buffer solution (PBS) was prepared by using Na_2HPO_4 and KH_2PO_4. 0.01 mM citrate buffer was prepared by using citric acid and trisodium citrate. All solutions were prepared using Milli-Q (Millipore, Bedford, MA, USA) A-10 gradient (18 MΩ cm) deionized water.

2.2. Apparatus

Electrochemical experiments were performed on an Electrochemical Analyzer (CHI 832, CH Instruments Co., USA) with a four-electrode cell consisting of the dual enzymatic-biosensor as working electrodes, a saturated calomel electrode (SCE) as reference electrode and a platinum-wire as auxiliary electrode. Two glassy carbon (GC, $d = 3$ mm) electrodes were used as the base electrodes for fabrication of the dual enzymatic-biosensor. Surface morphologies of the modified electrodes were investigated by scanning electron microscope (SEM, S-4800, Hitachi Instrument, Japan).

2.3. Experimental animals

Male Sprague–Dawley (SD) mice (3 weeks of age; 200 ± 20 g) were purchased from Shanghai Laboratory Animal Center, Chinese Academy Sciences and adapted for 3 weeks under temperature- and humidity-controlled conditions. The animals were housed in plastic cages under 12 h light:12 h dark cycle, and given free access to drinking water and a basal diet. The animals of diabetic group were given intraperitoneal injections of the freshly prepared STZ (60 mg kg^{-1} in 0.01 mM citrate buffer) within 5 min to induce diabetics, while animals of normal control group were only injected with buffer. After injection, serum glucose level was determined within 2 weeks, and mice with serum glucose level in the range of 250–400 mg dL^{-1} were included in study group ($n = 4$). Control mice had normal glucose level of less than 125 mg dL^{-1} ($n = 4$). Animals were sacrificed at 16 weeks old (after 2 months of diabetes). The experimental protocol was carried out in accordance with the Guide for the Care and Use of Laboratory Animals [23].

2.4. Cells and serum collection

PMs were harvested from the peritoneal fluid of mice by intraperitoneal injection of PBS. The cell suspension were plated and incubated in a humidified incubator (5% CO_2, 95% air) for 2 h at 37 °C The non-adherent cells were removed by washing three times with pre-warmed 0.1 M PBS (pH 7.14) and the adherent macrophages were incubated with Dulbecco's modified Eagle's medium (DMEM) containing 10% BSA for 24 h in a humidified atmosphere (CO_2, 95% air) at 37 °C. At the end of 24 h incubation period, the macrophage-conditioned media were washed three times with 0.1 M PBS (pH 7.14), centrifugated at a speed of 1500 rpm for 15 min at 4 °C and removed the supernatant. Then the PMs were suspended in 1 mL of 0.1 M PBS.

Blood samples of the experimental mice were drawn from animals' eye vein after collection of PMs. Serum was prepared by centrifugation at a speed of 1500 rpm for 20 min after standing for 25 min at room temperature, and collected the supernatant.

All samples were frozen at −20 °C until processed immediately.

2.5. Preparation of the dual enzymatic-biosensor

Prior to surface modification, two GC electrodes were polished with 0.05 μm alumina followed by successive sonication in acetone and deionized water. Afterwards, PTH was electrochemically deposited on the two GC electrodes via potential cycling in a range of −0.4 and +1.2 V (versus SCE) at a scan rate of 50 mV s^{-1} for 30 cycles in a 0.1 M H_2SO_4 aqueous solution containing 0.5 mM thionine. Two PTH/GC modified electrodes were then drop-coated 10 μL GNPs colloid, respectively. After being air-dried and rinsed with deionized water, one GNPs/PTH/GC modified electrode was transferred into PBS (pH 7.0), which contains 1.0 mg of GOx and 2.5% CH. Then GOx/GNPs/PTH/GC modified electrode (i.e. glucose sensor)

was achieved. Similarly, ChOx-ChE/GNPs/PTH/GC modified electrode (i.e. cholesterol sensor) was obtained through immersing the other GNPs/PTH/GC modified electrode into PBS containing 1.0 mg of ChE, 1.0 mg of ChOx and 2.5% of CH. After about 3 h at room temperature, the two enzymatic-modified electrodes were rinsed with deionized water and stored in PBS (pH 7.0) at 4 °C until used.

2.6. Amperometric determination of glucose and cholesterol in MPs and serum of mice

Firstly, the PMs suspensions were sonicated in ice bath at 600 W for 6 × 4 s to break cells, and determined the protein contain by improved Lowry method [24]. Then, the suspensions were added 7.2% TCA to precipitate protein and centrifugated at a speed of 1500 rpm for 5 min. The concentrations of glucose and cholesterol in the resulting PMs and serum supernatant were determined using the following procedures. Amperometric measurement experiments were carried out in a four-electrode system using CHI 832 electrochemical system. The dual biosensor was acted as two working electrodes, a SCE as reference electrode and a platinum-wire as auxiliary electrode. The applied potential was −0.2 V. The current measurements were performed in a home-built experimental system containing 10 mL of 0.1 M PBS (pH 6.5). After a steady-state background current baseline was obtained, 10 μL of the PMs or serum supernatant were injected into 10 mL PBS (pH 6.5) buffer solution and then the current response was recorded subsequently. All measurements were performed at room temperature. The concentrations of glucose and cholesterol were obtained using the calibration curves, which will be described later in Section 3.

3. Results and discussion

3.1. Electrodeposition of PTH and properties of the PTH/GC modified electrode

Prior to immobilization of enzymes and GNPs, GC electrodes were modified by electropolymerization of thionine. The polymer PTH could be employed as ETM to shuttling electrons between the redox centers of GOx or ChOx and the GC electrode. The cyclic voltammograms (CV) for electrodeposition of PTH layer (Fig. 1A) showed a monotonic increment in the reduction and oxidation peak currents, at approximately +0.246 V and +0.276 V, respectively. These results indicated the gradual growth of the electroactive polymer via radical dimerization routine [25]. The polymerization-experienced electrodes were then cycled from −0.4 to 0.6 V in 0.1 M PBS (pH 6.5) at a scan rate of 80 mV s^{-1} (Fig. 1B). Compared with the bare GC electrode, the PTH/GC modified electrode exhibited a couple of redox waves with the formal potentials of −0.24 V and −0.18 V, and the peak-to-peak separation (ΔE_p) value of 60 mV was close to the expected Nernst value of 59 mV for a two-electron/two-proton process.

3.2. Characterization of the enzymatic biosensor by SEM

The typical SEM images of GNPs/PTH/GC and GOx/GNPs/PTH/GC modified electrodes are shown in Fig. 2. It can be observed that the fibroid PTH was well cross-linked on the electrode surface, and the GNPs with estimated dimensions of 10 nm in diameter were absorbed closely on the surface of PTH (Fig. 2A). After the immobilization of GOx, the surface of the GNPs/PTH/GC modified electrode underwent an apparent change and was covered with GOx (Fig. 2B). A similar SEM image could be observed from the ChOx-ChE/GNPs/PTH/GC modified electrode.

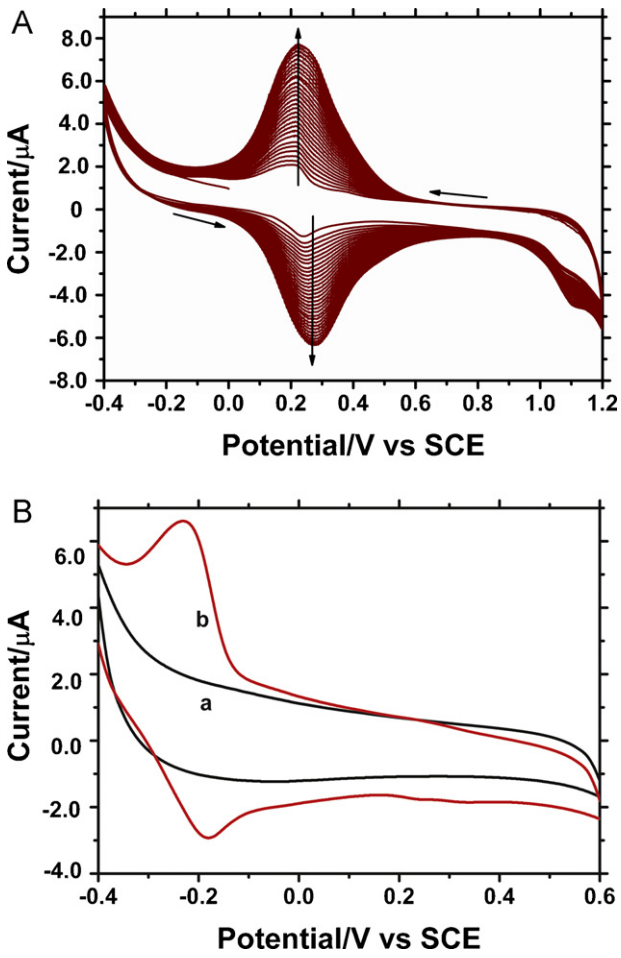

Fig. 1. (A) Electrodeposition of PTH via cycling in a range of −0.4 and +1.2 V (versus SCE) at a scan rate of 50 mV s^{-1} for 30 cycles in a 0.1 M H_2SO_4 aqueous solution containing 0.5 mM thionine. (B) CVs of (a) bare GC electrode, (b) PTH/GC modified electrode in a range of −0.4 and +0.6 V (versus SCE) at a scan rate of 80 mV s^{-1} in 0.1 M PBS (pH 6.5).

3.3. Electrochemical characteristics of the enzymatic biosensor

The electrochemical properties of the enzymatic biosensor were studied by electrochemical impedance spectroscopy (EIS) and CV, which were performed in 0.1 M PBS (pH 7.4) containing 2.5 mM $Fe(CN)_6^{3-}/Fe(CN)_6^{4-}$ (1:1). EIS, as an effective method to probe the interface features of surface-modified electrodes, confirmed the electrical communication between the redox probe $Fe(CN)_6^{3-/4-}$ and the electrode upon the stepwise modification process (Fig. 3A). The alternating voltage was 5 mV and the frequency range was 0.1–100 kHz. In the curve of the EIS, the semicircular corresponds to the electron-transfer-limited process and its diameter is equal to the electron transfer resistance (R_{et}) at the electrode surface [26]. As shown in Fig. 3A, significant differences were observed during stepwise modification. At the bare GC electrode, the redox process of the probe showed a R_{et} of about 175 Ω (curve a), while the PTH/GC modified electrode exhibited a larger R_{et} for the redox probe (curve b), because of the electrostatic repulsion between negatively charged surface of the PTH layer and the probe molecule. With further immobilization of GNPs onto the PTH/GC modified electrode (curve c), the R_{et} decreased, which indicated that GNPs had good conductivity and could make electron transfer easier. Subsequently, the R_{et} increased drastically once GOx was immobilized on GNPs (curve d), due to the hindrance provided by macromolecular configuration of

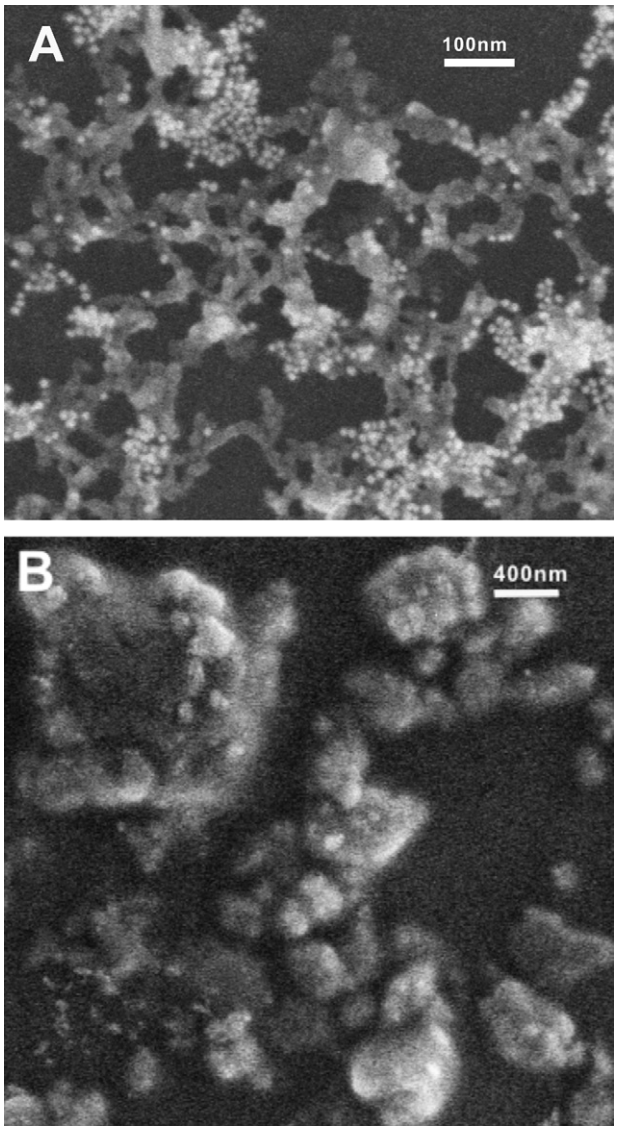

Fig. 2. SEM images of (A) the GNPs/PTH/GC and (B) the GOx/GNPs/PTH/GC modified electrodes.

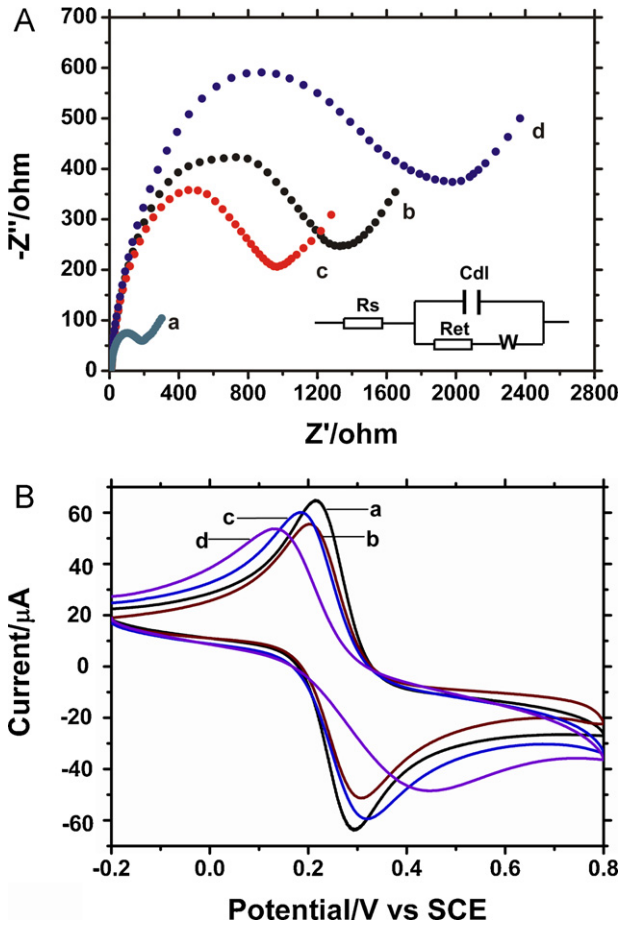

Fig. 3. (A) The Nyquist plots of the electrochemical impedance spectroscopy (EIS) for (a) bare GC, (b) PTH/GC, (c) GNPs/PTH/GC, (d) GOx/GNPs/PTH/GC modified electrodes in PBS (pH 7.4) containing 2.5 mM $Fe(CN)_6^{3-}/Fe(CN)_6^{4-}$ (1:1) by applying a voltage with 5 mM amplitude in a frequency range from 0.1 Hz to 100 kHz. The electrode potential was −0.5 V versus SCE. The inset is the Randles equivalent circuit for the modified electrodes. (B) CVs of (a) bare GC, (b) PTH/GC, (c) GNPs/PTH/GC, (d) GOx/GNPs/PTH/GC modified electrodes in PBS (pH 7.4) containing 2.5 mM $Fe(CN)_6^{3-}/Fe(CN)_6^{4-}$ (1:1) at 50 mV s^{-1}.

GOx to electron transport between electrode and redox mediator. The similar EIS could be obtained during the fabrication of the ChOx-ChE/GNPs/PTH/GC modified electrode. CV was further used to study the changes of the electrode behavior after each assembly step and the results were in agreement with those from EIS (Fig. 3B).

3.4. Electrochemical behaviors of the dual enzymatic-biosensor

Amperometric measurement was carried out for the simultaneous determination of glucose and cholesterol, which can be made by combining two enzymatic reactions with the electrochemical oxidation of the ETM. As shown in Scheme 1, both GOx and ChOx contain a kind of redox active center, flavin adenine dinucleotide (FAD), which can catalyse glucose or cholesterol to gluconolactone or 4-cholestene-3-one homologously. Meanwhile, the oxidized FAD of GOx and ChOx is reduced to $FADH_2$. Then the lost electrons of two enzymes are transferred to electrodes in the reversible, two-electron and two-proton transfer process of PTH film. The final current responses corresponded to the concentrations of glucose and cholesterol, respectively.

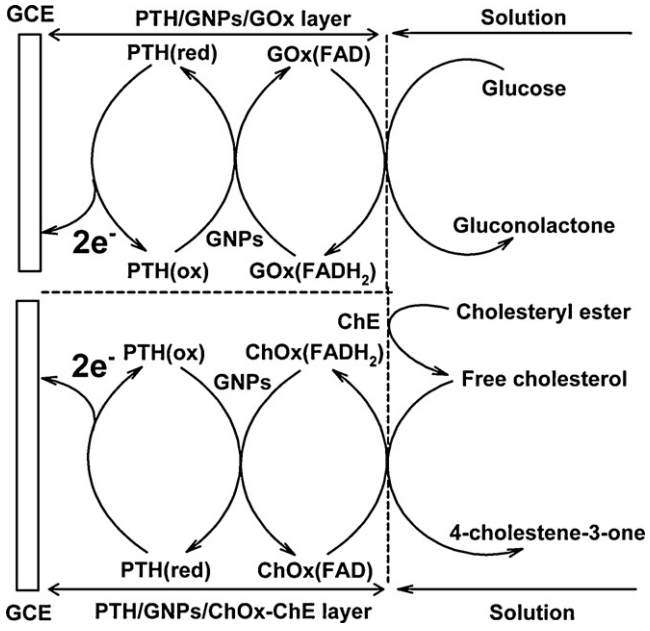

Scheme 1. Schematic illustration of the dual enzymatic-biosensor for electrochemical analysis of glucose and cholesterol simultaneously.

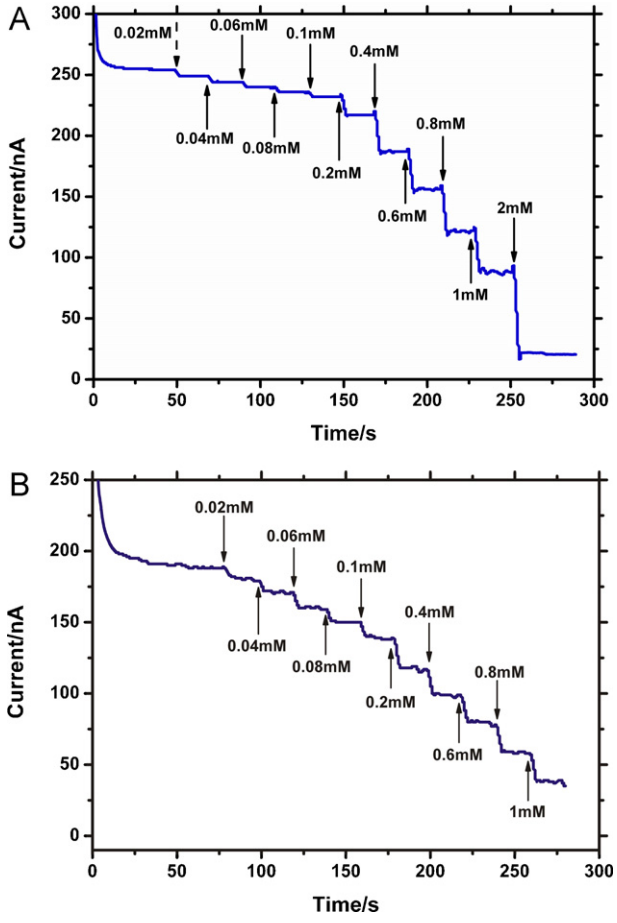

Fig. 4. Amperometric response of glucose sensor to various concentrations of glucose (A), and amperometric response of cholesterol sensor to various concentrations of cholesterol oleate (B), in stirred PBS (pH 6.5) at −0.2 V.

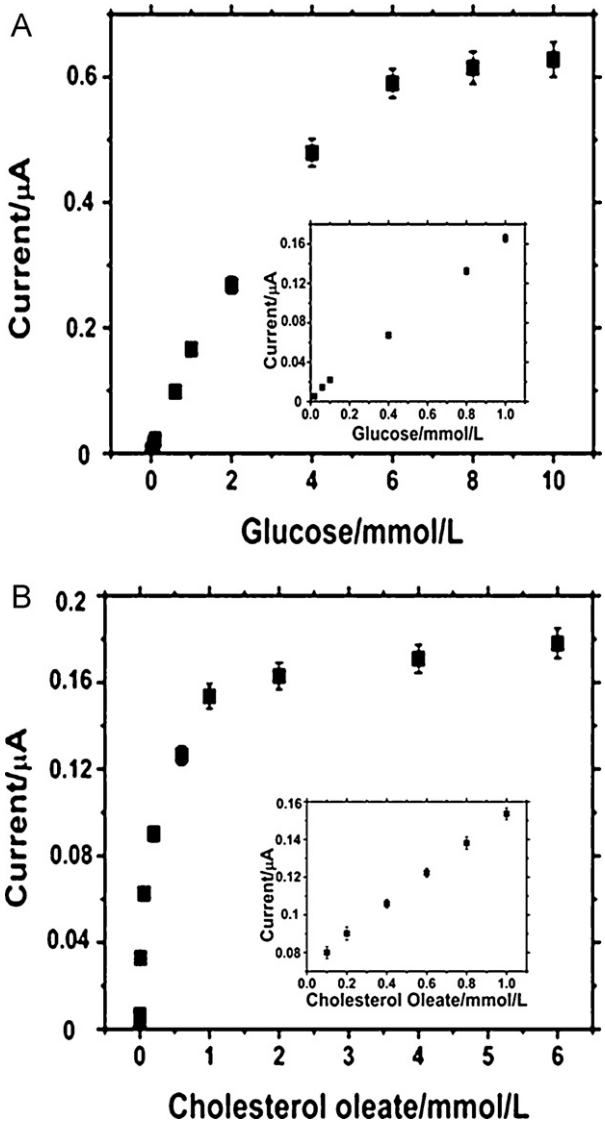

Fig. 5. Calibration plots for glucose at glucose sensor (A) and cholesterol at cholesterol sensor (B). Insets: calibration plots for glucose (A) and cholesterol oleate (B) from 0 to 1 mM. Each data point and error bar represents the mean and SD of 12 replicate measurement.

Fig. 4 shows the amperometric responses of the developed glucose and cholesterol sensors to various concentrations of glucose and cholesterol in PBS (pH 6.5) at −0.2 V. It was observed that the oxidation currents of glucose and cholesterol sensors were increased with the increasing concentration of glucose and cholesterol successively.

The calibration curves for glucose and cholesterol sensors are presented in the insets of Fig. 5. The glucose sensor shows a linear response over a wide concentration range from 0.008 mM to 6.0 mM with a linear correlation coefficient of 0.9987, and a detection limit of 2.0 μM based on signal-to-noise ratio of 3. The linear calibration range of cholesterol sensor is from 0.002 mM to 1.0 mM with a linear correlation coefficient of 0.9983, and a detection limit of 0.6 μM based on signal-to-noise ratio of 3. The high sensitivity could be attributed to the introduction of the GNPs on the film of PTH/GC modified electrode which could increase the catalytically electroactive surface area and act as tiny conduction centers to facilitate the electron transfer between enzymes and electrodes.

By the Lineweaver–Burke form of the Michaelis–Menten equation, the apparent Michaelis–Menten constants (K_M^{app}) can be calculated to characterize the enzyme reaction kinetics. The K_M^{app} of the glucose and cholesterol sensors were equal to 0.8689 mM of glucose and 0.0886 mM of cholesterol, respectively. Both of the values were comparable to the reported values, indicating that the enzymes (GOx, ChOx and ChE) retained their highly functional bioactivity and high biological affinity to glucose, cholesterol and cholesterol oleate after the immobilization [27–30]

3.5. Selectivity, reproducibility and stability of the dual enzymatic-biosensor

The selectivity of biosensor plays a crucial role in their application to the biological sample analysis. To affirm the selectivity of the proposed dual enzymatic-biosensor, possible interference of AA and UA on the current response of the glucose and cholesterol sensors was shown in Fig. 6. The amperometric response to successive additions of 20 μM UA and 20 μM AA were insignificant, which resulted in less than 4% deviations from both glucose (0.5 mM) and cholesterol (0.5 mM). The negligible interference on the current response of enzyme catalysis may be due mainly to the negative working potential provided by PTH. Moreover, the possible crosstalk between the dual biosensor was also determined, and the results were displayed in Fig. 5. In the presence of 60 μM UA and 60 μM AA, 0.5 mM cholesterol oleate and glucose were successively added to the solution. It can be seen that the cholesterol sensor exhibited an excellent response to cholesterol oleate and a very slight response to glucose; while the glucose sensor showed a good response to glucose and a very little response to cholesterol

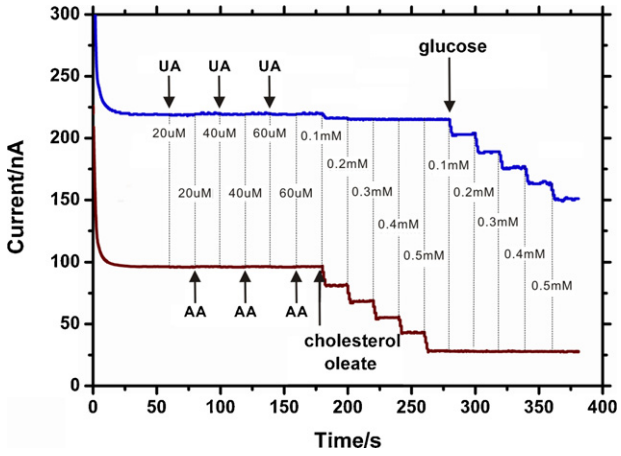

Fig. 6. Current–time response at the electrochemical biosensors toward UA (20 μM, 40 μM, 60 μM, 80 μM) and AA (20 μM, 40 μM, 60 μM, 80 μM), cholesterol oleate (0.1 mM, 0.2 mM, 0.3 mM, 0.4 mM, 0.5 mM), and glucose (0.1 mM, 0.2 mM, 0.3 mM, 0.4 mM, 0.5 mM) in 0.1 mM PBS (pH 6.5) at −0.2 V.

oleate. These obtained results strongly demonstrated that the dual enzymatic-biosensor bear little crosstalk from each other.

The reproducibility of the proposed method was estimated by repetitively measuring glucose (0.2 mM) and cholesterol oleate (0.2 mM) at the dual enzymatic-biosensor for five times. The results indicated that the method possessed a good reproducibility with relative standard deviation of 4.3% for the glucose sensor and 3.6% for the cholesterol sensor. The storage stability of the dual enzymatic-biosensor was also determined by measuring change in the current response at regular interval of 3 days for 4 weeks. When not used, the dual enzymatic-biosensor was stored in PBS at 4 °C. The results indicated that 89.2% of the response current of the glucose sensor and 88.7% of the response current of the cholesterol sensor were retained after three weeks.

3.6. Real sample analysis

In real sample studies, the glucose and cholesterol concentrations in serum and PMs from diabetic and non-diabetic mice were simultaneously analyzed with the proposed dual enzymatic-biosensor. In the test, 10 μL of real sample was injected into 10 mL PBS (pH 6.5) buffer solution as the detection solution. The sample was diluted 1000 times. The linear ranges for glucose and cholesterol could satisfy the determination of the diluted real sample. The quantitative levels of real samples after conversion were listed in Table 1. As shown in Table 1, the concentrations of serum glucose and cholesterol in non-diabetic mice averaged as 6.54 ± 0.29 mM and 1.92 ± 0.04 mM, respectively. For STZ-induced diabetic mice, the serum glucose concentration raised to 3.3-fold of control (21.5 ± 0.93 mM), but the serum cholesterol concentration had no significant change compared to the net increase of the serum glucose concentration. These results agree with the phenomenon that serum cholesterol in a large percentage of DM patients does not increase with elevated serum glucose level [31,32]. Moreover, in diabetic mice, the PMs glucose concentration was 3.58-fold of control, averaged as 139.31 ± 18.14 mM mg^{-1} cell protein, and the PMs cholesterol concentration was 2.14-fold of control, averaged 24.55 ± 1.31 mM mg^{-1} cell protein, which showed obvious difference to that of the serum cholesterol level. In conclusion, for diabetic mice, the serum glucose concentration was evidently higher than that of control and there was no significant increase in serum cholesterol concentration. The relationship between glucose and cholesterol in diabetic serum seemed to be independent, which may lead to chance of the risk of diabetes-accelerated

Table 1
Determination of glucose and cholesterol in serum and PMs from non-diabetic and diabetic mice.

Mice		C (serum glucose, mM)			C (serum cholesterol, mM)			C (PMs glucose, Mm mg^{-1} cell protein)			C (PMs cholesterol, mM mg^{-1} cell protein)		
		Individual	Mean	S.D.	Individual	Mean	S.D.	Individual	Mean	S.D.	Individual	Mean	S.D.
Non-diabetic mice	1	6.60 ± 0.29	6.54 ± 0.22	0.18	1.92 ± 0.07	1.92 ± 0.03	0.02	39.22 ± 1.96	38.92 ± 1.94	1.60	11.7 ± 0.58	11.48 ± 0.57	0.56
	2	6.32 ± 0.26			1.89 ± 0.06			37.11 ± 1.85			10.8 ± 0.54		
	3	6.76 ± 0.33			1.95 ± 0.07			40.94 ± 2.05			12.1 ± 0.61		
	4	6.49 ± 0.28			1.91 ± 0.06			38.39 ± 1.91			11.3 ± 0.56		
Diabetic mice	5	22.2 ± 1.13	21.53 ± 0.07	0.58	2.24 ± 0.12	2.24 ± 0.04	0.02	144.53 ± 7.23	139.31 ± 5.56	11.4	25.5 ± 1.27	24.55 ± 0.95	0.83
	6	20.8 ± 1.04			2.21 ± 0.10			123.75 ± 6.18			23.6 ± 1.18		
	7	21.4 ± 1.07			2.27 ± 0.12			138.65 ± 6.93			24.2 ± 1.21		
	8	21.7 ± 1.09			2.25 ± 0.10			150.31 ± 7.52			24.9 ± 1.24		

atherosclerosis. While in PMs of diabetic mice, the glucose concentration and the cholesterol concentration were remarkably higher than that of controls. The cooperative change in diabetic PMs suggests that glucose and cholesterol might play important roles in diabetes-accelerated atherosclerosis development. It has been reported that the high macrophage cholesterol content can induce macrophage foam cell formation, which is the hallmark of early atherosclerosis. These findings indicated the possibility that high glucose induced by diabetes could increase the macrophage cholesterol level and further accelerate atherosclerosis development, which is in agreement with the previous report [4].

4. Conclusions

This work has demonstrated the fabrication of a dual enzymatic-biosensor for simultaneous determination of glucose and cholesterol in serum and PMs of diabetic mice. The dual enzymatic-biosensor was established by immobilizing GOx and ChE/ChOx onto GNPs/PTH/GC modified electrodes, respectively. PTH coupled with GNPs could provide the dual biosensor with high anti-interferant, good sensitivity and stability. The fabricated dual enzymatic-biosensor was satisfactory in simultaneous determination of glucose and cholesterol in serum and PMs of mice. The results we obtained demonstrated that the relationship of glucose and cholesterol in diabetic PMs plays an important role in the development of diabetes-accelerated atherosclerosis.

Acknowledgements

This work was financially supported by the National Natural Science Foundation of China (Nos. 20775026 and 21075041), Science and Technology Commission of Shanghai Municipality (No. 1052nm06500).

References

[1] J. Stamler, O. Vaccaro, J. Neaton, D. Wentworth, Diabetes Care 16 (1993) 434–444.
[2] S.M. Grundy, Am. J. Cardiol. 81 (1998) 18B–25B.
[3] M.I. Uusitopa, L.K. Niskanen, O. Siitonen, E. Voutilainen, K. Pyörälä, Circulation 82 (1990) 27–36.
[4] T. Hayek, M. Kaplan, R. Kerry, M. Aviram, Atherosclerosis 195 (2007) 277–286.
[5] P. Hery, F. Thomas, A. Benetos, L. Guize, Hypertension 40 (2002) 458–463.
[6] L. Jiang, H. Liu, J. Liu, Q. Yang, X. Cai, J. Electroanal. Chem. 619-620 (2008) 11–16.
[7] V. Shumyantseva, G. Deluca, T. Bulko, S. Carrara, C. Nicolini, S. Usanov, A. Archakov, Biosens. Bioelectron. 19 (2004) 971–976.
[8] X.L. Luo, J.J. Xu, Y. Du, H.Y. Chen, Anal. Biochem. 334 (2004) 284–289.
[9] G. Li, J.M. Liao, G.Q. Hu, N.Z. Ma, P.J. Wu, Biosens. Bioelectron. 20 (2005) 2140–2144.
[10] S.B. Bankar, M.V. Bule, R.S. Singhal, L. Ananthanarayan, Biotechnol. Adv. 27 (2009) 489–501.
[11] R. Maidan, A. Heller, Anal. Chem. 64 (1992) 2889–2896.
[12] N. Takahiro, K. Susumu, Y. Hiroshi, Anal. Chem. 69 (1997) 2367–2372.
[13] C.A. Groom, J.H.T. Luoung, Biosens. Bioelectron. 9 (1994) 305.
[14] J.J. Rippeth, PhD Thesis, University of Leeds, 1998.
[15] L. He, C.S. Toh, Anal. Chim. Acta 556 (2006) 1–15.
[16] X. Ren, X. Meng, F. Tang, L. Zhang, Mater. Sci. Eng. C 29 (2009) 2234–2238.
[17] J.L. Besombes, S. Cosnier, P. Labbe, Talanta 44 (1997) 2209–2215.
[18] J.L. Besombes, S. Cosnier, P. Labbe, G. Reverdy, Anal. Chim. Acta 317 (1995) 275–280.
[19] A. Gantman, B. fuhrman, M. Avriam, T. Hayek, Biochem. Biophys. Res. Commun. 391 (2010) 523–528.
[20] K. Marielle, K. Rachel, A. Michael, H. Tony, J. Cardiovasc. Pharmacol. 52 (2008) 324–332.
[21] J.P. Mauldin, S. Srinivasan, A. Mulya, A. Gebre, J.S. Parks, A. Daugherty, C.C. Hedrick, J. Biol. Chem. 281 (2006) 21216–21224.
[22] N. Zhou, J. Wang, T. Chen, Z.G. Yu, G.X. Li, Anal. Chem. 78 (2006) 5227–5230.
[23] Committee on Care and Use of Laboratory Animals, Guide for the Care and Use of Laboratory Animals, Institute of Laboratory Animal Resources, National Research Council, Washington, DC, 1985, pp. 83.
[24] O.H. Lowry, H.J. Rosembrough, L. Farr, R. Randall, J. Biol. Chem. 193 (1951) 263–275.
[25] J.M. Bauldreay, M.D. Archer, Electrochim. Acta 28 (1983) 1515–1522.
[26] A.C. Dillon, T. Gennett, K.M. Jones, J.L. Alleman, P.A. Parilla, M.J. Heben, J. Adv. Mater. 11 (1999) 1354–1358.
[27] T. Ferri, S. Maida, A. Poscia, R. Santucci, Electroanalysis 13 (2001) 1198–1202.
[28] A. Kumar, R.R. Pandey, B. Brantley, Talanta 69 (2006) 700–705.
[29] S. Singh, R. Singhal, B.D. Malhotra, Anal. Chim. Acta 582 (2007) 335–343.
[30] A.S. Santos, A.C. Pereira, M.D.P.T. Sotomayor, R.T. Tarley, D. Duran, L.T. Kubota, Electroanalysis 19 (2007) 549–554.
[31] R.C. Turner, H. Millns, H.A.W. Neil, I.M. Stratton, S.E. Manley, D.R. Matthews, R.R. Holman, BMJ 316 (1998) 868–873.
[32] H. Jemai, A.E. Feki, S. Sayadi, J. Agric. Food Chem. 57 (2009) 8798–8804.